A new mutation in a family with cold-aggravated myotonia disrupts Na^+ channel inactivation

F.–F. Wu, BS; M.P. Takahashi, MD, PhD; E. Pegoraro, MD, PhD; C. Angelini, MD; P. Colleselli, MD; S.C. Cannon, MD, PhD; and E.P. Hoffman, PhD

Article abstract—*Objective:* To identify the molecular and physiologic abnormality in familial myotonia with cold sensitivity, hypertrophy, and no weakness. *Background:* Sodium channel mutations were previously identified as the cause of several allelic disorders with varying combinations of myotonia and periodic paralysis. A three-generation family with dominant myotonia aggravated by cooling, but no weakness, was screened for mutations in the skeletal muscle sodium channel α-subunit gene (*SCN4A*). *Methods:* Single-strand conformation polymorphism was used to screen all 24 exons of *SCN4A* and abnormal conformers were sequenced to confirm the presence of mutations. The functional consequence of a *SCN4A* mutation was explored by recording sodium currents from human embryonic kidney cells transiently transfected with an expression construct that was mutated to reproduce the genetic defect. *Results:* A three-generation Italian family with myotonia is presented, in which a novel *SCN4A* mutation (leucine 266 substituted by valine, L266V) is identified. This change removes only a single methylene group from the 1,836-amino-acid protein, and is present in a region of the protein previously not known to be critical for channel function (domain I transmembrane segment 5). Electrophysiologic studies of the L266V mutation showed defects in fast inactivation, consistent with other disease-causing *SCN4A* mutations studied to date. Slow inactivation was not impaired. *Conclusions:* This novel mutation of the sodium channel indicates that a single carbon change in a transmembrane α-helix of domain I can alter channel inactivation and cause cold-sensitive myotonia.

NEUROLOGY 2001;56:878–884

Skeletal muscle sodium channelopathies are a group of dominantly inherited disorders that present with a variable combination of myotonia, periodic paralysis, and exacerbating triggers.[1-3] Before the discovery of a common gene defect for these allelic disorders, several clinical syndromes were delineated. Recurrent attacks of weakness in association with elevated serum potassium are the hallmarks of hyperkalemic periodic paralysis (HyperPP). Myotonia may also be present, but episodic weakness is the predominant symptom. Myotonia that paradoxically worsens with continued muscular activity (paramyotonia) and is exacerbated by cooling is the cardinal feature of paramyotonia congenita (PC). Patients with PC may also have spontaneous or cold-induced attacks of severe generalized weakness, but paramyotonic stiffness is typically the chief complaint in affected patients.

Additional material related to this article can be found on the *Neurology* Web site. Go to www.neurology.org and scroll down the Table of Contents for the April 10 issue to find the title link for this article.

The term potassium-aggravated myotonia (PAM) has been used to designate another clinical entity within this group of allelic sodium channelopathies. PAM is characterized by myotonia that often fluctuates temporally and may be either mild or severely debilitating. As implied by the name, potassium administration often produces dramatic worsening of myotonic stiffness. Paramyotonia is not a feature of PAM, and by definition, patients with PAM do not have episodic weakness or dystrophy. Many clinical variants of sodium-channel–based myotonia are now considered to be forms of PAM: myotonia fluctuans, myotonia permanens, acetazolamide-responsive myotonia, and painful myotonia. Although these disorders are clinically distinct in exemplary cases, atypical symptoms, overlapping signs and clinical variability often preclude a definitive diagnosis within this scheme.

To date, 24 missense mutations have been identified and all mutations studied cause a gain-of-function of the sodium channel, with impaired fast

From the Department of Human Genetics (F.-F. Wu), University of Pittsburgh, PA; Departments of Neurology (Drs. Takahashi and Cannon) and Neurobiology (Dr. Cannon), Massachusetts General Hospital, Harvard Medical School, Boston, MA; Neuromuscular Unit, Department of Neurological and Psychiatric Sciences (Drs. Pegoraro and Angelini), University of Padova, Italy; Division of Pediatrics (Dr. Colleselli), ULSS n.1 Belluno Agordo Cadore, O.C. di Belluno, Belluno, Italy; and the Research Center for Genetic Medicine (F.-F. Wu and Dr. Hoffman), Children's National Medical Center, Washington, DC.

This work was supported by grants from the NIH (E.P.H. and S.C.C.), Sumitomo Life Insurance Welfare Services Foundation (M.P.T.), and Telethon grant C41 for tissue bank (C.A.). E.P.H. is an Established Investigator of the American Heart Association.

Received May 24, 2000. Accepted in final form December 13, 2000.

Address correspondence and reprint requests to Dr. Eric P. Hoffman, Research Center for Genetic Medicine, Children's National Medical Center, 111 Michigan Avenue NW, Washington, DC 20010; e-mail: ehoffman@childrens-research.org

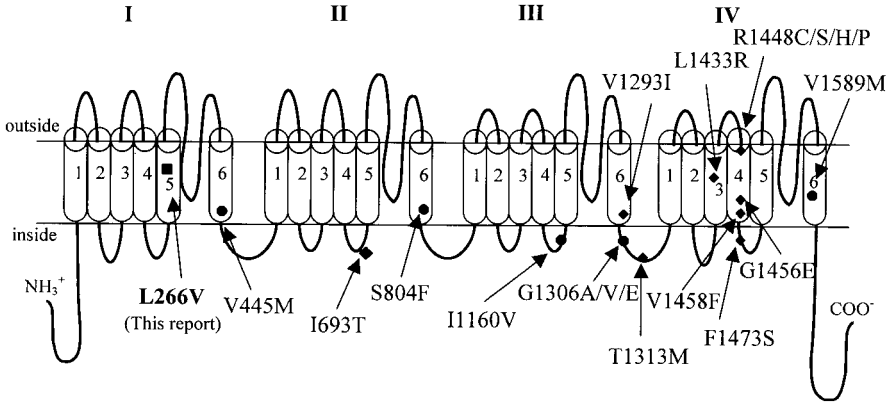

Figure 1. The skeletal muscle sodium channel α-subunit and mutations identified in patients with paramyotonia congenita (♦) and potassium-aggravated myotonia (●). The L266V mutation (■) is in the fifth transmembrane segment of domain I.

inactivation and for some, enhanced activation.[2,3] *SCN4A* is a member of the voltage-gated sodium channel gene family. There are 12 genes identified to date in this family, which show dispersed expression in CNS, peripheral nervous system, heart, muscle, and electrically excitable tissues throughout different species.[4] The structure of the voltage-gated sodium channel α-subunit contains four homologous domains, each consisting of six transmembrane segments.[5] The functional domains involved in channel activation, inactivation, and ion selectivity have been intensively studied biochemically, electrophysiologically, and pharmacologically.[6] Early studies showed that the cytoplasmic loop between domains III and IV serves a gating function for fast inactivation and that clustered, positively charged amino acids in the fourth transmembrane segment of each domain function as voltage sensors. However, mutation studies in humans and horses affected with PC, HyperPP, and PAM have greatly extended the number of regions that can alter inactivation.[3] Among the 24 *SCN4A* mutations identified to date, the majority of changes have been found clustered in domains III and IV (figure 1). These regions are important for coupling depolarization to fast inactivation of the channels.

We report a family with dominant myotonia aggravated by cold and not associated with weakness in which we identified a new missense mutation in the fifth transmembrane segment of domain I.

Methods. *Clinical data.* The index case was 11 years old when he was first evaluated for persistent muscle stiffness provoked and worsened by cooling, but also present under warm conditions. The parents reported that he had shown ocular myotonia and hand stiffness since he was 9 months old. Myotonic attacks affected muscles of the distal upper extremities more severely than those of the legs, face, and neck. The patient denied symptoms of myalgia, spontaneous episodes of muscle weakness, or exercise-induced weakness. He had frequent cramps in the hands when writing and attacks of uncontrolled eye closure lasting 10 to 30 seconds in cold weather. The patient reported that when playing soccer outdoors the myotonia could involve the leg muscles, but prolonged activity did not result in a further aggravation of stiffness (no paramyotonia). Neurologic exam at age 16 years showed a mild lordosis with muscle hypertrophy more evident in the lower extremities. Muscle strength was normal. Percussion myotonia was absent, although hints of action myotonia were present in the orbicularis oculi. An electromyographic study done at age 16 showed widespread myotonic discharges in all muscles tested. After cooling electromyography showed spontaneous discharges of high-frequency potentials of variable amplitude from 0.05 to 0.5 mV in the cooled muscles. Echocardiogram and EKG were normal. Serum creatine kinase was mildly elevated (530 U/L; normal, <200 U/L).

The proband's father reported similar symptoms of myotonia with onset in his teens, with stiffness in the arms, hands, face, and neck. He reported that his fingers would become increasingly stiff and immobile in cold weather. He denied any symptoms in the lower limbs. Neurologic exam at age 48 years showed a diffuse muscular hypertrophy and lid lag phenomenon with preserved muscle strength. No warm-up phenomenon was observed. Neither emotional stress nor specific food intake worsened or provoked onset of myotonic attacks in the proband or his father.

The index case's paternal uncle, paternal aunt, and paternal grandmother were all reported to show cold-induced muscle stiffness, with no muscle weakness. These three individuals were presumed to be affected but were not clinically examined.

DNA studies. Genomic DNA was extracted from 10 mL of whole blood collected in purple top blood collection tube (ethylenediaminetetraacetic acid [EDTA]) as previously described.[7] Patient DNA samples were first screened for two common *SCN4A* mutations, T704M and M1592V, by amplification-refractory mutation system analysis.[8] Single-strand conformation polymorphism (SSCP) mutation screening was then done for all 24 exons of *SCN4A* as previously described.[9] PCR products showing conformers by SSCP were reamplified and purified by QIAquick PCR purification kit (QIAGEN, Hilden, Germany). Purified PCR products were then subjected to automated sequence analysis using BigDye™ terminator (PE Biosystems, Foster City, CA) and analyzed on an ABI PRISM 377 sequencer (PE Biosystems, Foster City, CA). Data were analyzed using Sequencher™ 3.0 program (Gene Codes Corporation, Ann Arbor, MI). The identified mutation abolished a HinP1 I restriction enzyme site in exon 6. Exon 6 was amplified in 65 normal control DNA samples (total

130 chromosomes) and tested for the presence of HinP1 I restriction fragments.

Site-directed mutagenesis. The QuikChange™ site-directed mutagenesis kit (Stratagene, La Jolla, CA) was used to introduce the L266V mutation into the human skeletal muscle sodium channel mammalian expression construct pRc/CMV-hSkM1 provided by A.L. George, Jr.[10] This vector contains the 6.1-kb *SCN4A* complementary DNA (cDNA) in the pRc/CMV vector (Invitrogen, Carlsbad, CA). Clones were sequenced around the mutation site to confirm the presence of the mutation, and to ensure that no other mutations were generated during the site-directed mutagenesis process.

Expression of sodium channels. Culture of human embryonic kidney (HEK) cells and their transient transfection were performed as described previously.[11] In brief, normal (wild-type [WT]) or mutant (L266V) sodium channel α-subunit plasmid (0.9 μg/35-mm dish) was cotransfected with a β_1-subunit plasmid (fourfold molar excess over α-subunits) and a CD8 marker (0.175 μg/35-mm dish) using the calcium phosphate method. The human β_1-subunit cDNA[12] was subcloned into the EcoRI site of the mammalian expression vector pcDNA1[13] (Invitrogen). After 48 to 72 hours, HEK cells were trypsinized briefly and passaged to 22-mm round glass coverslips for electrophysiologic recording. Individual transfection-positive cells were identified by labeling with anti-CD8 antibody cross-linked to microbeads[14] (Dynal, Great Neck, NY).

Whole-cell recording. Na^+ currents were measured using conventional whole-cell recording techniques as described previously.[11] Recordings were made with an Axopatch 200A amplifier (Axon Instruments, Foster City, CA). The output was filtered at 5 kHz and digitally sampled at 40 kHz using an LM900 interface (Dagan, Minneapolis, MN). Data were stored on a Pentium-based (Intel, Santa Clara, CA) computer using a custom AxoBasic (Axon Instruments) data acquisition program. More than 80% of the series resistance was compensated by the analog circuitry of the amplifier and the leakage conductance was corrected by digital scaling and subtraction of the passive current elicited by a 20-mV depolarization from the holding potential. Cells with peak currents of <1 nA or >20 nA upon step depolarization from −100 mV to −10 mV were excluded. After initially establishing whole-cell access, we often observed leftward shifts in the voltage dependence of gating, an increase in the size of the peak current, and a decrease in the amplitude of persistent Na^+ current. To minimize these effects, we waited at least 10 minutes for equilibration after gaining access to the cells.

Patch electrodes were fabricated from borosilicate capillary tubes with a multistage puller (Sutter, Novato, CA). The shank of the pipette was coated with Sylgard and the tip was heat-polished to a final tip resistance (in bath solution) of 0.5 to 2.0 MΩ. The pipette (internal) solution contained 105 mM CsF, 35 mM NaCl, 10 mM EGTA, and 10 mM Cs-HEPES (pH 7.4). Fluoride was used in the pipette to prolong seal stability. The bath solution contained 140 mM NaCl, 4 mM KCl, 2 mM $CaCl_2$, 1 mM $MgCl_2$, 5 mM glucose, and 10 mM Na-HEPES (pH 7.4). Recordings were made at room temperature (21 to 23 °C).

Data analysis. Curve fitting was performed manually off-line using AxoBasic or Origin (Microcal, Northampton, MA) programs. Conductance was calculated as G(V) = I_{peak} (V)/(V − E_{rev}), where the reversal potential, E_{rev}, was measured experimentally for each cell. The voltage dependence of activation was quantified by fitting the conductance measures to a Boltzmann function $G(V) = G_{max}/[1 + \exp(-(V - V_{1/2})/k)]$. Steady-state fast and slow inactivation were fitted to a Boltzmann function with a nonzero pedestal, I_0, calculated as $I/I_{peak} = (1 - I_0)/[1 + \exp((V - V_{1/2})/k)] + I_0$, where $V_{1/2}$ is the half-maximum voltage and k is the slope factor. Symbols with error bars indicate means ± SEM in figures 4 and 5.

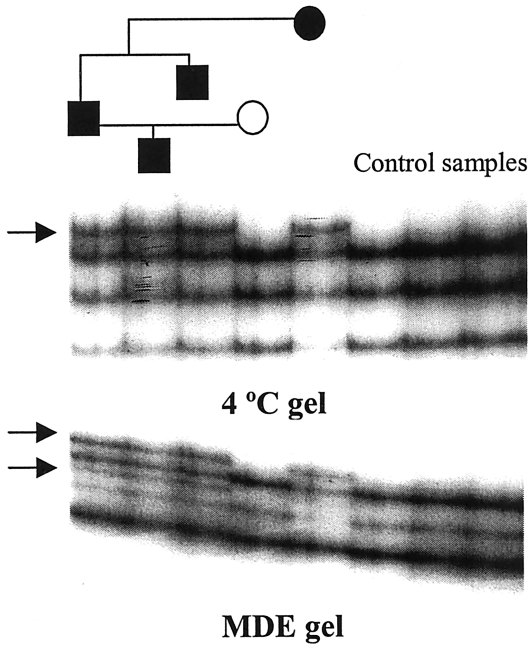

Figure 2. Single-strand conformation polymorphism (SSCP) analysis of exon 6 of SCN4A *in cold room and MDE gel conditions. Arrows indicate aberrant bands detected in the Italian patients.*

Results. *Molecular genetic analyses.* DNA samples from the Italian family with cold-aggravated myotonia were screened for *SCN4A* mutations by SSCP. Unique conformers in exon 6 were seen in both cold room and MDE gels (FMC Corporation, Rockland, ME) (figure 2). Sequencing of the unique conformers showed a C to G transversion at coding sequence position 796 in the affected family members but not in normal control subjects (figure 3A). This change abolished one of the two HinP1 I restriction enzyme sites in exon 6, resulting in characteristic restriction enzyme digestion patterns shown in figure 3B. None of 65 normal control DNA samples (a total of 130 chromosomes) showed this change by HinP1 I restriction enzyme digestion (data not shown).

Fast inactivation. The kinetics of Na^+ channel gating were characterized by recording whole-cell currents from HEK cells transiently transfected with cDNA encoding the β_1-subunit and either WT or mutant (L266V) sodium channel protein. Cells were held at −100 mV and Na^+ currents were elicited by a series of 10-ms step depolarizations from −75 to +75 mV in 5-mV increments. Figure 4A shows whole-cell Na^+ currents for WT and L266V, normalized to the maximal current amplitude. On average, there was no difference in peak current amplitude for cells expressing

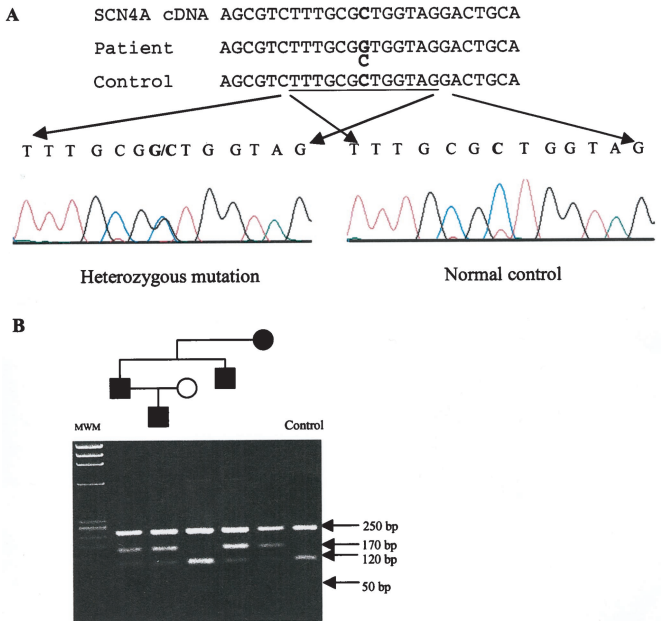

Figure 3. Identification of a L266V change in the Italian family. (A) DNA sequencing results. The patient's genomic DNA shows a heterozygous C→G mutation resulting in the L266V amino acid change. (B) HinP1 I restriction enzyme digestion patterns of the Italian family and normal control subject show all affected individuals to be heterozygous for this change.

L266V mutants (8.1 ± 1.2 nA; n = 17) compared with WT channels (8.0 ± 1.2 nA; n = 23). L266V differed from WT currents with slower decay of macroscopic currents. To illustrate this difference more clearly, current traces at −10 mV are superimposed for WT and L266V (figure 4A, right). In this example, the current decayed three times more slowly for L266V (1.75 ms) than WT (0.58 ms).

The voltage-dependence of steady-state inactivation (availability) was measured as the peak current elicited following a 300-ms conditioning prepulse. Figure 4B, left (squares) shows the voltage dependence of the steady-state relative availability for WT and L266V. The data from L266V were shifted rightward (depolarized) and were less steep compared with WT. To quantify this difference, the data were fitted with a Boltzmann function. For L266V channels, the average for the midpoint of the curve ($V_{1/2}$) was shifted +12 mV ($p < 0.0003$) and the slope factor (k) was 1.2-fold larger (WT [n = 23] $V_{1/2}$ = −73.3 ± 0.8 mV and k = 4.9 ± 0.2 mV; L266V [n = 17] $V_{1/2}$ = −61.4 ± 1.2 mV and k = 5.8 ± 0.2 mV).

The kinetics of fast inactivation was characterized by quantifying the time course of entry to and recovery from inactivation. Entry at depolarized potentials (−30 to + 30 mV) was measured by fitting the decay of sodium current with a single exponential (see figure 4C [triangles]). A defect in fast inactivation for the L266V mutant was discernible at voltages above −20 mV as a two- to threefold slower time constant. Over an intermediate range of voltages, −70 to −40 mV, the time course of fast inactivation was measured using a two-pulse protocol. First, a conditioning pulse depolarization was applied for 1 to 100 ms. Inactivation was measured as a decrease in the peak Na^+ current elicited by the second pulse to −10 mV. The relative Na^+ current as a function of conditioning pulse duration was fitted with a single exponential, and the time constants were plotted against the conditioning pulse voltage in figure 4C (squares). At −60 and −70 mV, the time constant for inactivation from closed states was two- to threefold faster for L266V than for WT (n = 7 to 8; $p <$ 0.005).

We measured the time course of recovery from the fast-inactivated state at more hyperpolarized range of voltages (−120 to −80 mV) using a two-pulse protocol. A 30-ms conditioning pulse to −10 mV was applied to fully fast-inactivate the channel. The membrane was then hyperpolarized for 0.05 to 2,000 ms, and then recovery was monitored by measuring the relative peak Na^+ current elicited by second pulse to −10 mV. The recovery of the peak amplitude was fitted with a single exponential and the time constants are shown vs the recovery potential in figure 4C (circles). Over the voltage range studied, recovery of the peak current was 1.8 to 3.3 times faster for L266V than for WT (n = 7 to 9; $p < 0.00001$). The depolarized shift in the $V_{1/2}$ of availability, the faster rate of recovery, and the slower rate of entry are all indicative of disrupted fast inactivation for L266V.

Mutations may also disrupt the completeness of fast inactivation, which is detected as an anomalous Na^+ current that persists for several tens of milliseconds after the test depolarization.[15] Because even a small persistent Na^+ current can alter the excitability of the cell, a subtraction protocol was used to detect the presence of Na^+ currents on the order of 0.2% of the initial inward peak transient. The current elicited by a 50-ms step depolarization from −100 mV to −10 mV was measured with control solution and in the presence of a saturating concentration of tetrodotoxin (5 μM). The difference between the two responses is a sensitive measure of the current conducted only through Na^+ channels. The amplitude of the steady-state current during the last 5 ms of the pulse was averaged and normalized to the amplitude of peak transient current. There was no significant persistent Na^+ current at −10 mV for L266V channels (0.07 ± 0.06% [n = 4]) compared with WT (−0.006 ± 0.07). Both were indistinguishable from 0 ($p < 0.4$).

Activation. Sodium channel activation was characterized by measuring the voltage dependence of the peak Na^+ conductance. Na^+ currents were elicited using a series of step depolarizations as in figure 4A. The Na^+ conductance was estimated from the peak current and the measured reversal potential (see "Methods" section), and its voltage dependence is plotted in figure 4B right (circles). The conductance data were fit with a Boltzmann function. There was no difference in the estimated parameter values: WT (n = 23) $V_{1/2}$ = −26.6 ± 0.8 mV and k = 5.6 ± 0.3 mV; L266V (n = 17) $V_{1/2}$ = −26.7 ± 0.9 mV and k = 5.1 ± 0.3 mV. The reversal of activation upon repolarization is termed *deactivation* and this process was reportedly impeded by PC mutations at position R1448.[16] We measured the rate of deactivation by first opening channels with a 0.5 ms step to −10 mV and then promoting deactivation by stepping back to voltages ranging from −70 to −100 mV. There was no difference in the time constant of the current decay (WT [n = 5] = 0.056 ± 0.004 ms; L266V [n = 4] = 0.054 ± 0.012 ms at −90 mV), which implies that deactivation was not affected.

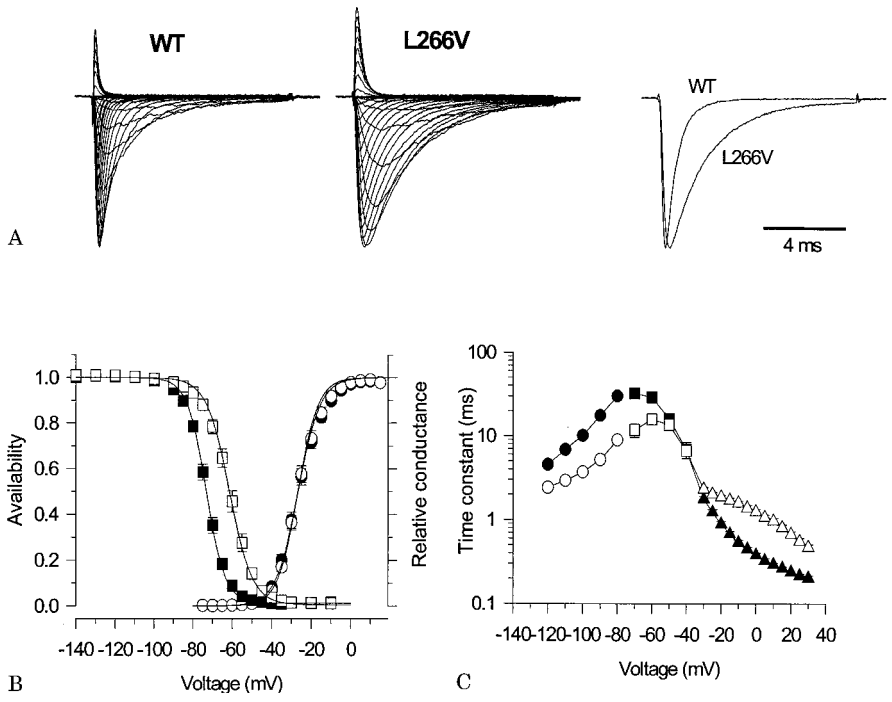

Figure 4. Fast inactivation is impaired in sodium channels containing the L266V change. (A) Sodium currents were elicited for wild-type (WT) and L266V channels by applying a series of 10-ms depolarization steps (5-mV increment from −75 to +75 mV) from a holding potential of −100 mV (left). Current amplitudes were normalized by the maximal peak amplitude; 6.2 nA for WT, 5.1 nA for L266V. Current traces at −10 mV were superimposed for comparison of the macroscopic current decay in WT and L266V (right). The time constant for relaxation was approximately threefold slower for L266V (1.75 ms) compared with WT (0.58 ms). (B) The voltage dependence of availability (steady-state fast inactivation, left, squares) and conductance (right, circles) are shown for WT and L266V. The voltage dependence of steady-state fast inactivation was measured as the relative peak Na^+ current elicited at −10 mV after application of a 300-ms conditioning pulse. Fitting the steady-state fast inactivation data to a Boltzmann function, $I/I_{max} = 1/[1 + \exp((V - V_{1/2})/k)]$, showed a significant depolarized (rightward) shift for L266V: WT (■) $V_{1/2} = -73.3 \pm 0.8$ mV and $k = 4.9 \pm 0.2$ mV; L266V (□) $V_{1/2} = -61.4 \pm 1.2$ mV and $k = 5.8 \pm 0.2$ mV. The voltage-dependence of the conductance, $G(V) = I_{peak}/(V - E_{rev})$, was determined from the peak current, I_{peak}, measured with the same protocol in (A). Conductance values for each cell were normalized to the maximum value and the relative conductance was fitted to a Boltzmann function. The estimated parameters were similar: WT (●) $V_{1/2} = -26.6 \pm 0.8$ mV and $k = 5.6 \pm 0.3$ mV; L266V (○) $V_{1/2} = -26.7 \pm 0.9$ mV and $k = 5.1 \pm 0.3$ mV. (C) The voltage dependence of the kinetics of fast inactivation is shown by combining data from two-pulse recovery (−120 to −80 mV; WT [●], L266V [○]), two-pulse entry (−70 to −40 mV; WT [■], L266V [□]), and single-pulse relaxation (entry) protocols (>−30 mV; WT [▲], L266V [△]). Each symbol denotes the protocol used to measure the time constant.

Slow inactivation. The voltage dependence of slow inactivation is shown for WT and L266V mutant channels in figure 5. Steady-state slow inactivation was measured using a 60-second prepulse followed by a 20-ms gap at −120 mV to allow recovery from fast inactivation, before the −10-mV test pulse (inset). Although the voltage dependence of slow inactivation in L266V channels was significantly steeper ($p < 0.002$), the voltage for half inactivation ($V_{1/2}$) and the maximal extent of slow inactivation (I_0) did not differ significantly: WT (n = 4) $V_{1/2} = -66.8 \pm 1.8$ mV, $k = 10.2 \pm 0.4$ mV, and $I_0 = 0.10 \pm 0.004$; L266V (n = 6) $V_{1/2} = -65.3 \pm 2.0$ mV, $k = 6.54 \pm 0.6$ mV, and $I_0 = 0.08 \pm 0.01$.

Discussion. Most *SCN4A* mutations that have been identified in families showing dominant myotonia are clustered in domains III or IV of the sodium channel protein. The L266V mutation we report here is only the second disease-associated mutation found in domain I (see figure 1). This amino acid change shortens the aliphatic side chain by only a single hydrocarbon, yet we show causality of this mutation by a variety of approaches. First, the mutation followed the disease in the family. Second, the change was not seen in 130 normal chromosomes. Third, the Leu266 residue is conserved throughout evolution from *Electrophorus electricus* to *Rattus norvegicus* to *Homo sapiens*, and is also preserved in different sodium channel isoforms expressed in diverse tissues (additional information can be found on the *Neurology* Web site, www.neurology.org). Most importantly, we show a functional abnormality of the L266V sodium channel by whole-cell recording of heterologously expressed channels.

Mutant L266V sodium channels showed slowed macroscopic current inactivation, an accelerated recovery rate, and a depolarized shift in the steady-state voltage dependence (see figure 4). We believe these functional defects of fast inactivation cause myotonia for several reasons. First, all of the alterations in fast inactivation behavior result in a gain-of-function wherein mutant channels conduct more inward Na^+ current than normal (WT) channels. The anomalous inward Na^+ current would depolarize the fiber and thereby increase excitability. The shift of inactivation toward more depolarized potentials (see figure 4B) may also help prevent attacks of depolarization-induced weakness. Second, similar functional defects have been reported for other myotonia-associated Na^+ channel mutations. Third,

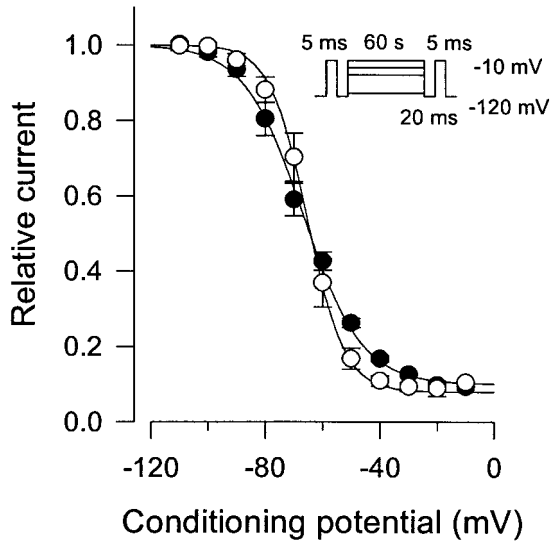

Figure 5. The voltage dependence of slow inactivation is similar for wild-type (WT) and L266V mutation channels. The fraction of Na^+ channels not undergoing slow inactivation was measured as the peak current elicited at −10 mV after a 60-s conditioning pulse (inset). Current amplitudes were normalized to the reference peak current elicited from a holding potential of −120 mV. The conditioning and test pulses were separated by a 20-ms hyperpolarization to −120 mV to allow channels to recover from fast but not slow inactivation. Smooth curves show fits of the data by a Boltzmann function plus a constant term; WT (n = 4) (●) $V_{1/2}$ = −66.8 ± 1.8 mV, k = 10.2 ± 0.4 mV, and I_0 = 0.10 ± 0.004; L266V (n = 6) (○) $V_{1/2}$ = −65.3 ± 2.0 mV, k = 6.54 ± 0.6 mV, and I_0 = 0.08 ± 0.01.

these functional defects have been shown in model simulation to be sufficient to cause the self-sustained bursts of action potentials that cause myotonia.[17]

To date, seven missense mutations of the skeletal muscle sodium channel associated with PAM and 11 with PC have been reported. Fast gating behavior has been characterized for 16. As in the present study of L266V, the Na^+ current decay was markedly slowed for other mutations causing prominent myotonia.[10,18-20] Also consistent with several reports for myotonic mutations, we found an accelerated recovery from fast inactivation.[10,16,18-21] For L266V channels, steady-state fast inactivation was shifted to depolarized direction, although the direction of shift has been reported to differ among Na^+ channel mutations associated with myotonia.[10,18,20]

Impaired fast inactivation by L266V mutation is of particular interest due to the very subtle change on the protein structure, and also due to its unusual position in the sodium channel protein. Only one of the other 24 disease-associated missense mutations occur in domain I.[13,22] Indeed, the functional deficits that we observed for the L266V mutations were rather unexpected. Mutations in S5 segments of the other homologous domains (II and IV) were recently shown to similarly affect fast inactivation. A HyperPP-associated mutation in S5 of domain II, T704M, also shifts steady-state fast inactivation in the depolarized direction,[18] although this shift was not confirmed in subsequent studies.[23] Another HyperPP mutation in S5 of domain IV, I1495F, also slows the macroscopic current decay and produces a hyperpolarized shift in steady-state fast inactivation.[23] Slow inactivation of the skeletal muscle Na^+ channel was recently recognized as an additional determinant in the propensity for periodic paralysis.[24] Slow inactivation is partially impaired in some but not all mutations that cause HyperPP.[24,25] Conversely, defects in slow inactivation have never been identified in functional studies of skeletal muscle sodium channel mutations associated with pure myotonia without weakness. Because the family described here with the L266V mutation did not have muscle weakness, our data demonstrating no dramatic defect in slow inactivation further support the association of clinical attacks of weakness with functional defects in slow inactivation.

The clinical features of this family included symptoms considered atypical for paramyotonia congenita. The proband and his father had cold-induced myotonia, but there were no signs of paramyotonia. Instead, the proband described a "warm-up–like" phenomenon involving the muscles of lower limbs. The "warm-up–like" phenomenon could not be elicited during clinical evaluation, however. Other atypical features were persistent myotonia under warm conditions, and diffuse muscle hypertrophy. The findings from this family clearly emphasize the difficulty of distinguishing the various forms included in the large spectrum of sodium channelopathies. We believe that this family's clinical features are most consistent with a variant of PAM. Cold-aggravated myotonia is known to occur in PAM,[26] and the absence of paramyotonia or weakness further supports this diagnosis. PAM may be confused with myotonia congenita (chloride channel disorder), although the latter typically shows muscle hypertrophy. The muscle hypertrophy seen in our family further enlarges the clinical spectrum of sodium channelopathies.

Acknowledgment

The authors thank the Italian family members for participating in this study and Jim Giron and Dr. Francisco Martínez-Murillo for their technical support of mutation studies.

References

1. Hoffman EP, Lehmann–Horn F, Rüdel R. Overexcited or inactive: ion channels in muscle disease. Cell 1995;80:681–686.
2. Lehmann–Horn F, Jurkat-Rott K. Voltage-gated ion channels and hereditary disease. Physiol Rev 1999;79:1317–1372.
3. Cannon SC. Spectrum of sodium channel disturbances in the nondystrophic myotonias and periodic paralyses. Kidney Int 2000;57:772–779.
4. Goldin AL. Diversity of mammalian voltage-gated sodium channels. Ann NY Acad Sci 1999;868:38–50.
5. Catterall WA. Structure and function of voltage-sensitive ion channels. Science 1988;242:50–61.

6. Catterall WA. From ionic currents to molecular mechanisms: the structure and function of voltage-gated sodium channels. Neuron 2000;26:13–25.
7. Higuchi R. Rapid, efficient DNA extraction for PCR from cells or blood. In: Amplifications: a forum for PCR users. Emeryville, CA: Cetus; 1989.
8. Newton CR, Graham A, Heptinstall LE, et al. Analysis of any point mutation in DNA. The amplification refractory mutation system (ARMS). Nucleic Acids Res 1989;17:2503–2516.
9. Orita M, Iwahana H, Kanasawa H, Hayashi K, Sekiya T. Detection of polymorphisms of human DNA by gel electrophoresis as single-strand conformation polymorphisms. Proc Natl Acad Sci USA 1989;86:2766–2770.
10. Chahine M, George AL Jr, Zhou M, et al. Sodium channel mutations in paramyotonia congenita uncouple inactivation from activation. Neuron 1994;12:281–294.
11. Hayward LJ, Brown RH, Jr., Cannon SC. Inactivation defects caused by myotonia-associated mutations in the sodium channel III-IV linker. J Gen Physiol 1996;107:559–576.
12. McClatchey AI, Cannon SC, Slaugenhaupt SA, Gusella JF. The cloning and expression of a sodium channel β_1-subunit cDNA from human brain. Hum Mol Genet 1993;2:745–749.
13. Takahashi MP, Cannon SC. Enhanced slow inactivation by V445M: a sodium channel mutation associated with myotonia. Biophys J 1999;76:861–868.
14. Jurman ME, Boland LM, Lin Y, Yellen G. Visual identification of individual transfected cells for electrophysiology using antibody-coated beads. Biotechniques 1994;17:874–881.
15. Cannon SC, Brown RH Jr, Corey DP. A sodium channel defect in hyperkalemic periodic paralysis: potassium-induced failure of inactivation. Neuron 1991;6:619–626.
16. Featherstone DE, Fujimoto E, Ruben PC. A defect in skeletal muscle sodium channel deactivation exacerbates hyperexcitability in human paramyotonia congenita. J Physiol 1998;506:627–638.
17. Cannon SC, Brown RH Jr, Corey DP. Theoretical reconstruction of myotonia and paralysis caused by incomplete inactivation of sodium channels. Biophys J 1993;65:270–288.
18. Yang N, Ji S, Zhou M, et al. Sodium channel mutations in paramyotonia congenita exhibit similar biophysical phenotypes in vitro. Proc Natl Acad Sci USA 1994;91:12785–12789.
19. Mitrovic N, George AL Jr, Heine R, et al. K^+-aggravated myotonia: destablization of the inactivated state of the human muscle Na^+ channel by the V1589 mutation. J Physiol 1994; 478:395–402.
20. Bendahhou S, Cummins TR, Kwiecinski H, Waxman SG, Ptacek LJ. Characterization of a new sodium channel mutation at arginine 1448 associated with moderate paramyotonia congenita in humans. J Physiol 1999;518:2.:337–344.
21. Green DS, George AL Jr, Cannon SC. Human sodium channel gating defects caused by missense mutations in S6 segments associated with myotonia: S804F and V1293I. J Physiol 1998; 510:685–694.
22. Rosenfeld J, Sloan-Brown K, George AL Jr. A novel muscle sodium channel mutation causes painful congenial myotonia. Ann Neurol 1997;42:811–814.
23. Bendahhou S, Cummins TR, Tawil R, Waxman SG, Ptacek LJ. Activation and inactivation of the voltage-gated sodium channel: role of segment S5 revealed by a novel hyperkalemic periodic paralysis mutation. J Neurosci 1999;19:4762–4771.
24. Hayward LJ, Sandoval GM, Cannon SC. Defective slow inactivation of sodium channels contributes to familial periodic paralysis. Neurology 1999;52:1447–1453.
25. Hayward LJ, Brown RH Jr, Cannon SC. Slow inactivation differs among mutant Na^+ channels associated with myotonia and periodic paralysis. Biophys J 1997;72:1204–1219.
26. Heine R, Pika U, Lehmann-Horn F. A novel SCN4A mutation causing myotonia aggravated by cold and potassium. Hum Mol Genet 1993;2:1349–1353.